Electrostatic-Capacitive MEMS Force Sensors: A State-of-the-Art Review

Alessandro Nastro, *Member, IEEE*

***Abstract*—MEMS force sensors are used in a wide range of technical applications, spanning from industrial and biomedical to consumer and biological fields. Due to their widespread adoption in the market, significant efforts have been dedicated in researching and developing various transduction principles, sensing materials, and innovative mechanical designs. This review summarizes the most employed transduction principles for force sensing at the MEMS scale. Among these, electrostatic-capacitive MEMS force sensors are particularly well-suited for implementing closed-loop configurations, as they can integrate both capacitive sensing and electrostatic actuation within a single device thus keeping the system compact and favorably compatible with integrated circuit. Accordingly, this review focuses on the latest research in the literature on electrostatic-capacitive MEMS force sensors operating in both open-loop and closed-loop configurations. The working principles of both approaches are discussed, along with their respective advantages and disadvantages, and a comparison of state-of-the-art sensors in terms of resolution, sensitivity, and measurement range is provided. Finally, the review presents future perspectives, highlighting challenges and opportunities for MEMS force sensor development. The goal is to offer references that can aid in improving the design and performance of novel MEMS force sensors. [2025-0166]**

***Index Terms*—Capacitive, closed-loop configuration, electrostatic, feedback, force sensors, MEMS, open-loop configuration, review.**

I. Introduction

IN the International System of Units, force is a derived unit and is a fundamental physical measure on which many quantities are based on. Torque, pressure, and acceleration, to name a few, are force-based physical quantities [1] that have driven the development of various sensors and continue to drive advances in both traditional and emerging research fields, including physics, electronics, and biology [2].

The demand of force sensors in the industry market is projected to grow from USD 4.28 Billion in 2024 to USD 6.53 billion by 2032 [3]. This positive trend is also a consequence of the exploitation of Micro Electro-Mechanical Systems (MEMS) technology for force sensing. MEMS force sensors have pathed the way to accurately measure micro-forces, i.e. in the millinewton range and below, along with the typical MEMS advantages such as miniaturization, low power consumption, low cost, low weight, mass-production and chip integration [4].

The exploitation of MEMS for force measurement has pushed advances in different scenarios. Examples of MEMS

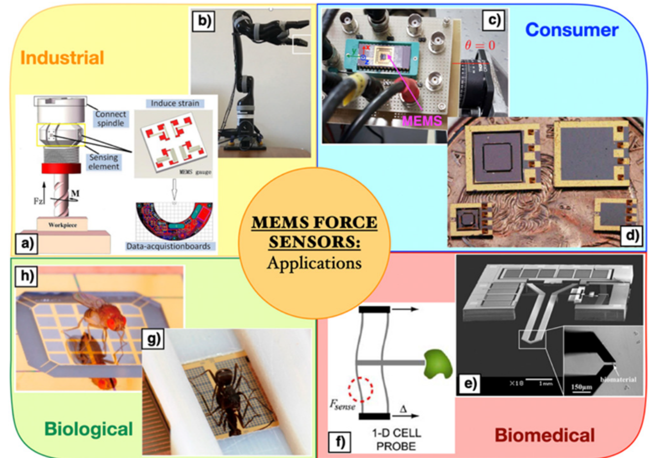

Fig. 1. Examples of MEMS force sensor applications. Industrial: (**a**) for milling process monitoring [5] and (**b**) for tactile sensation in robot [6]. Consumer: (**c**) as an inclinometer [7] and (**d**) as a pressure sensor [8]. Biomedical: (**e**) as a tool for cell manipulation [9] and (**f**) for investigation of cell mechanics [10]. Biological: (**g**) as sensors for locomotion and (**h**) gait inspections of insects [11].

force sensor exploitation in different research fields are shown in Fig. 1. In the industrial field, they have been employed to monitor the cutting force adopted during the milling process of a workpiece [5] and to develop next-generation robots having high-performance tactile sensation [6], as shown in Fig. 1a,b, respectively. In consumer applications, a MEMS inclinometer with electrically tunable angle sensitivity [7] and a MEMS pressure sensor able to withstand high temperature [8] have been developed exploiting force-based measurements as presented in Fig. 1c,d, respectively. MEMS force sensors have been successfully adopted in biomedical field to manipulate highly deformable biomaterials in an aqueous environment [9] and as tool for the advanced understanding of biological cell mechanics [10] as illustrated in Fig. 1e,f, respectively. In biological applications, MEMS devices for force sensing have been employed to investigate and analyze the movement and gait of insects [11] as shown in Fig. 1g,h, respectively.

Due to the wide spread of MEMS force sensors in the market, considerable effort has been made in harnessing different transduction principles, sensing materials, and innovative mechanical designs [12].

A common point in MEMS force sensors is that force sensing is typically achieved by converting the input force into a displacement or deflection by means of a movable or deformable mechanical structure characterized by a specific mechanical stiffness [13]. The displacement or deflection induced is then measured by employing a proper transduction

Received 9 September 2025; revised 20 November 2025; accepted 5 December 2025. Date of publication 16 December 2025; date of current version 5 February 2026. Subject Editor R. T. Howe.
The author is with the Department of Information Engineering, University of Brescia, 25123 Brescia, Italy (e-mail: alessandro.nastro@unibs.it).
Digital Object Identifier 10.1109/JMEMS.2025.3641973

© 2025 The Authors. This work is licensed under a Creative Commons Attribution 4.0 License.
For more information, see https://creativecommons.org/licenses/by/4.0/

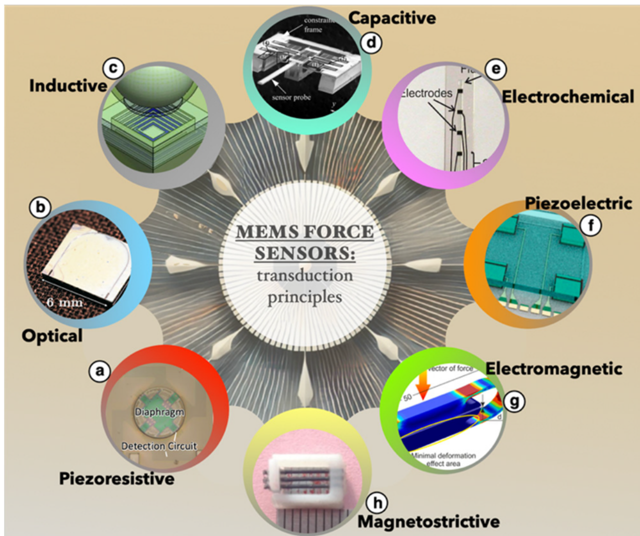

Fig. 2. Most commonly adopted transduction principles for MEMS force sensor: (**a**) piezoresistive [19], (**b**) optical [21], (**c**) inductive [23], (**d**) capacitive [24], (**e**) electrochemical [26], (**f**) piezoelectric [28], (**g**) electromagnetic [30] and (**h**) magnetostrictive [32].

principle. This kind of operation is denoted as *open-loop configuration* but, unfortunately, is prone to inaccuracies, range limitations and nonlinearities due to the intrinsic necessity to displace or deflect the sensor internal elastic structure for force detection [14]. To overcome this issue, the employment of an actuator can lead to a *closed-loop configuration* to keep the position of the internal elastic structure fixed thus offering higher accuracy and less perturbations from mechanical vibrations [15]. Closed-loop configuration can be expediently implemented in electrostatic-capacitive MEMS force sensors where the position of the internal elastic structure is sensed and actuated electrically [16]. These sensors typically rely on a capacitive displacement sensor and electrostatic actuators both integrated in the same device [17].

In this context, this review highlights the latest research developments focused on electrostatic-capacitive MEMS force sensors. Section II introduces different transduction principles that are typically employed in MEMS force sensors. Section III treats the electrostatic-capacitive transduction principle by describing MEMS force sensors available in the literature that implement open-loop and closed-loop configurations. Section IV accounts for conclusions and future perspectives.

II. MEMS Force Sensors Transduction Principles

In this section the most adopted transduction principles for mechanical force sensing in the MEMS scale are summarized by providing examples taken from the literature.

Piezoresistive force sensors can convert a mechanical force into a variation of electrical resistance by relying on the piezoresistive effect, that is defined as the change of resistance of semiconductors due to the applied mechanical stress [18]. Fig. 2a shows a MEMS hardness sensor aimed for medical applications based on a piezoresistive bridge circuit [19]. These sensors typically exhibit low production cost at the expense of high-power consumption and low repeatability [12].

Optical force sensors, and specifically fiber-based sensors, relate the change in period and in the refractive index distribution of a fiber grating with the external force applied to the sensor [20]. Fig. 2b shows an all-optical frequency modulated MEMS force sensor based on a mechanically amplified double clamped waveguide beam structure for harsh environments [21]. These sensors show good reliability and repeatability but are typically marked by high production cost.

Inductive force sensors rely on the change of magnetic coupling between a coil and a conductive force-sensitive target [22]. An inductive tactile sensor with a chrome steel ball sensing interface based on commercially available CMOS process is shown in Fig. 2c [23]. Inductive sensors typically show high linearity at the cost of demanding fabrication processes.

Capacitive force sensor relates the variation of electric capacitance to the force applied on a movable or deformable conductive mechanical electrode [12]. Fig. 2d shows a capacitive two-axis MEMS force sensor for biological studies at the cellular and organism levels [24]. Typically, capacitive force sensors require low power and have high force resolution but suffer of nonlinearities and measurement range limitations.

Electrochemical force sensors monitor changes to the ionic conduction path of current-carrying ions in the fluid register as a change in the magnitude of the solution impedance due to the application of an external force [25]. Fig. 2e shows a liquid-filled parylene-based microchannel and an array of electrodes able to monitor local variations in impedance during mechanical deformation of the channel [26]. The design and development of this sensor typology is demanding but in turn it exhibits biocompatibility and adaptability for aqueous and salty environments.

Piezoelectric force sensors detect the applied force by converting mechanical stress to electrical charges relying on the piezoelectric effect [27]. A force microsensor embedding a piezoelectric sensing layer for minimally invasive surgery is shown in Fig. 2f [28]. Due to the piezoelectric effect these sensors are not intended for static force measurements but exhibit high bandwidth.

Electromagnetic force sensors typically rely on the interrogation of a force-sensitive resonant element by the means of electromagnetic waves [29]. Fig. 2g shows an example of electromagnetic interrogation of a force sensor envisioned for the MEMS scale [30]. These sensors are still quite demanding in the MEMS scale but are prone to wireless interrogation approaches.

Magnetostrictive force sensors are based on materials that exhibit magnetic susceptibility change when subjected to external mechanical stress [31]. Fig. 2h shows a millimeter scale magnetostrictive sensor unit that employs permanent magnets, Fe-Ga wires, and Hall sensors for the detection of static and dynamic forces [32]. These sensors can withstand high mechanical overloads but, as for the electromagnetic force sensors, their exploitation in the MEMS scale remains challenging.

Regardless the transduction principle employed, MEMS force sensors typically rely on a movable or deformable mechanical structure on which the input force induces a

measurable displacement or deflection. An enhancement in MEMS force sensors can be achieved by not only measuring the moveable mechanical structure displacement but also actuating it to implement a closed-loop configuration. To this extent, electrostatic-capacitive MEMS force sensors exploit capacitive sensing and electrostatic actuation within the same MEMS device. Capacitance can be measured and controlled directly using standard electronic circuits, such as oscillators or capacitive bridges [33], without requiring complex conversion systems thus simplifying the design of the closed-loop configuration and reducing costs. Moreover, in a capacitive MEMS force sensor, the electrodes employed to measure the capacitance can also be used to induce electrostatic forces thus advantageously eliminating the need for separate actuators, keeping the system compact and favorably compatible with integrated circuit.

To this extent Section III highlights electrostatic-capacitive MEMS force sensors comparing performances of open and closed-loop configurations available in literature.

III. Electrostatic-Capacitive MEMS Force Sensor

As discussed in Section II, electrostatic-capacitive MEMS force sensors can rely on capacitive sensing and electrostatic actuation within the same device. Capacitive sensing is typically achieved by relating changes in the electric capacitance between two electrodes with the external force F_{ext}, which is usually exerted to a movable or deformable conductive mechanical component that serves as one of the electrodes. The capacitance value depends on the shapes and relative position of the electrodes as well as on the medium in which the electrodes are immersed [34]. The most widely employed capacitor typology is the parallel-plate configuration which capacitance C_{s}, neglecting the fringing effect, can be expressed as:

$$C_{\mathrm{s}} = \frac{\varepsilon A}{g} \tag{1}$$

where ε is the dielectric permittivity, A is the area of the facing electrodes and g is the gap between the electrodes. Typically, MEMS force sensors based on parallel-plate capacitors leverage on either the area or the gap dependence on F_{ext}, resulting in variable-gap or variable-area capacitors. Fig. 3a shows a schematic representation of a parallel-plate variable-gap capacitive sensor having a mechanically fixed electrode and a movable electrode both with length l_{s}. For variable-gap configuration the movable electrode displacement is assumed to be constrained to the y-direction. F_{ext} is applied to the movable electrode resulting in a variation of the gap. The equivalent capacitance C_{g} can be expressed as:

$$C_{\mathrm{g}} = \frac{\varepsilon t_{\mathrm{r}} l_{\mathrm{s}}}{y_0 - y_{\mathrm{Q}}} \tag{2}$$

where y_0 is the initial gap, t_{r} is the out-of-plane thickness and y_{Q} is the displacement along the y-direction that is function of F_{ext}. Electrodes are assumed with negligible width, and the fringe effect is neglected. The sensitivity S_{g} defined as the derivative of C_{g} with respect to y_{Q}, is:

$$S_{\mathrm{g}} = \frac{\mathrm{d}C_{\mathrm{g}}}{\mathrm{d}y_{\mathrm{Q}}} = \frac{\varepsilon t_{\mathrm{r}} l_{\mathrm{s}}}{\left(y_0 - y_{\mathrm{Q}}\right)^2} \tag{3}$$

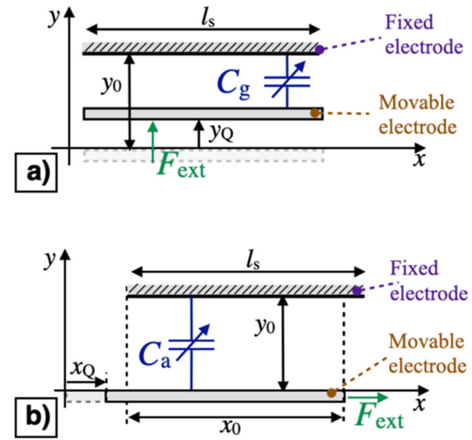

Fig. 3. Schematic representation of a variable-gap (**a**) and variable-area (**b**) parallel-plate capacitive sensor.

Fig. 3b shows a schematic representation of a parallel-plate variable-area capacitive sensor having a mechanically fixed electrode and a movable electrode both with length l_{s}. For variable-area configuration the movable electrode displacement is assumed to be constrained to the x-direction. F_{ext} is applied to the movable electrode resulting in a variation of the overlap length. The equivalent capacitance C_{a} can be expressed as:

$$C_{\mathrm{a}} = \frac{\varepsilon t_{\mathrm{r}} \left(x_0 + x_{\mathrm{Q}}\right)}{y_0} \tag{4}$$

where y_0 is the fixed gap between the electrodes, x_0 is the initial overlapping length, t_{r} is the out-of-plane thickness and x_{Q} is the displacement along the x-direction that is function of F_{ext}. The sensitivity S_{a} defined as the derivative of C_{a} with respect to x_{Q}, is:

$$S_{\mathrm{a}} = \frac{\mathrm{d}C_{\mathrm{a}}}{\mathrm{d}x_{\mathrm{Q}}} = \frac{\varepsilon t_{\mathrm{r}}}{y_0} \tag{5}$$

Eq. (3) and Eq. (5) show that for variable-gap capacitive sensor the sensitivity is a nonlinear function of the displacement that increases with decreasing the gap whereas for variable-area configuration it is constant with varying the displacement. Variable-area configuration has the advantage of exhibiting a linear function between the capacitance and the displacement and of having a fixed gap between the electrodes thus avoiding the pull-in instability [35]. However, having a constant sensitivity can possibly restraint the capacitance sensing range being limited to the physical size of the capacitor. The variable-gap configuration exhibits a broader capacitance sensing range, as its sensitivity can be increased by reducing the gap without altering the physical size of the capacitor.

Nevertheless, as shown in Eq. (2) the capacitance is a nonlinear function of the displacement, and the gap reduction can possibly lead to pull-in instability. Despite the drawbacks of both configurations and depending on the targeted application, either can be employed in MEMS force sensors as a *Force-to-Capacitance Converter* (FCC).

Electrostatic actuation in MEMS force sensors is typically achieved by relying on the electrostatic force F_{d} induced by applying a voltage between the electrodes of a capacitor. Specifically, the electrostatic actuation can be observed as the

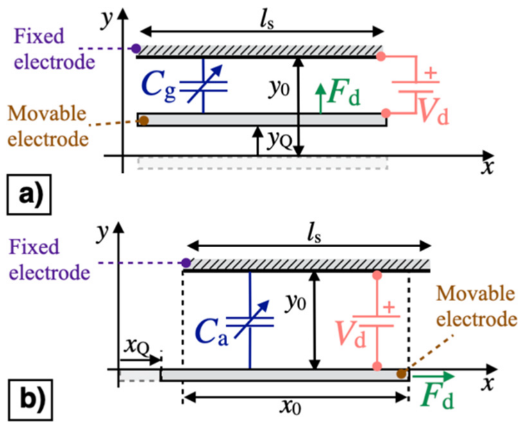

Fig. 4. Schematic representation of a variable-gap (**a**) and variable-area (**b**) parallel-plate electrostatic actuator.

force pulling together the two electrodes [36]. Fig. 4a shows a schematic representation of a parallel-plate variable-gap electrostatic actuator having the same geometrical parameters and constraints employed in Fig. 3a. By applying the voltage V_d between the electrodes the attractive electrostatic force F_d is generated and changes the displacement y_Q of the movable electrode. F_d can be derived from the energy $E = 1/2C_g V_d^2$ stored in the capacitor C_g as:

$$|F_d| = \frac{dE}{dy_Q} = \frac{\varepsilon t_r l_s}{2\left(y_0 - y_Q\right)^2} V_d^2 = \alpha_g V_d^2 \tag{6}$$

where α_g is an electromechanical conversion factor. Whereas Fig. 4b shows a schematic representation of a parallel-plate variable-area electrostatic actuator having the same constraints and geometrical parameters employed in Fig. 3b. By applying the voltage V_d between the electrodes the attractive electrostatic force F_d is generated and changes the displacement x_Q of the movable electrode. F_d can be derived from the energy $E = 1/2C_a V_d^2$ stored in the capacitor C_a as:

$$|F_d| = \frac{dE}{dx_Q} = \frac{\varepsilon t_r l_s}{2y_0} V_d^2 = \alpha_a V_d^2 \tag{7}$$

where α_a is an electromechanical conversion factor. Eq. (6) shows that for variable-gap electrostatic actuators both the electromechanical conversion factor and the electrostatic force increase with decreasing the gap. This can possibly lead at small gap to pull-in instability since the electrostatic force is unable to overcome the elastic restoring force, that is not shown in the schematic. While Eq. (7) shows that for variable-area electrostatic actuator both the electromechanical conversion factor and the electrostatic force are constant with varying x_Q. This allows to electrostatic actuate the movable electrode by exploiting a constant conversion factor which depends only on the capacitor geometrical parameters thus avoiding the pull-in instability. The exploitation of either variable-area or variable-gap electrostatic actuator allows to implement another key conversion stage for MEMS force sensors that is the *Voltage-to-Force Converter* (VFC). FCCs and VFCs are crucial converting stages adopted for the exploitation of open-loop and closed-loop configurations in static-mode force sensing.

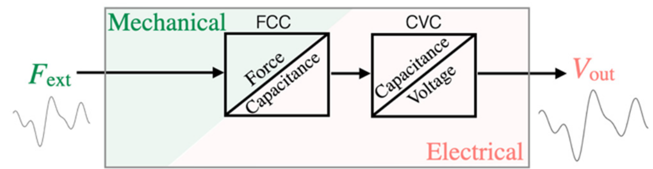

Fig. 5. Block diagram of a force sensor based on an open-loop configuration.

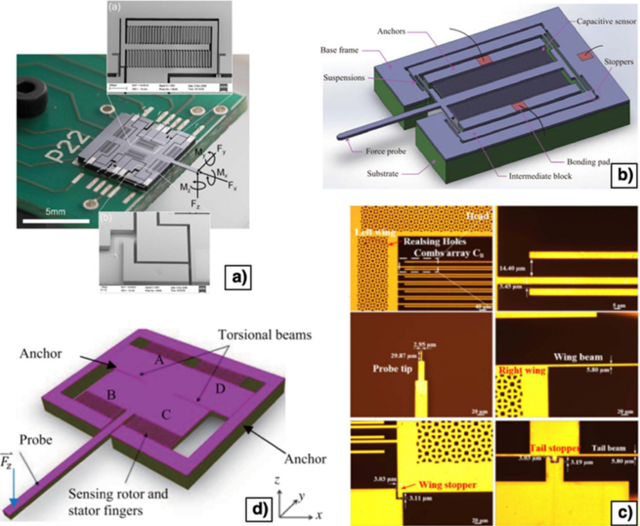

Fig. 6. Examples of capacitive MEMS force sensors available in literature having a probe tip suspended by springs: (**a**) a six-axis MEMS force sensor [37], (**b**) a MEMS force sensor with enhanced measurement range [38], (**c**) a single-axis MEMS force sensor [39] and (**d**) a CMOS-MEMS capacitive force sensor for out-of-plane force measurement [40].

A. Open-Loop Configuration

Fig. 5 shows a schematic representation of a force sensor exploiting an open-loop configuration. This configuration allows to obtain as output an electrical signal which is typically a voltage V_{out} function of the input mechanical signal, i.e., the external force F_{ext}. In its simplest form, the open-loop configuration embeds an FCC and a *Capacitance-to-Voltage Converter* (CVC) to convert F_{ext} from the mechanical domain into V_{out} in the electrical domain. Fig. 6 shows examples of capacitive MEMS force sensor employed in open-loop configuration. Fig. 6a shows a MEMS force sensor having a 3-mm long probe tip connected to a movable mass suspended by flexures that allow deflections and rotations along the three axes. The displacement is sensed by exploiting both variable-area and variable-gap capacitors [37]. Fig. 6b shows a uniaxial capacitive MEMS force sensor that leverages on mechanical stoppers to achieve distinctive stiffnesses and in turn different measurement ranges and resolutions [38].

A MEMS force sensor with a bio-inspired design is shown in Fig. 6c [39]. A single-axis MEMS force sensor designed for out-of-plane measurement is shown in Fig. 6d [40].

The majority of MEMS devices designed for force measurement, as the ones shown in Fig. 6, exhibit a probe tip suspended by springs on which F_{ext} is applied and a FCC based on variable-area or variable-gap capacitors. These devices can thus be described by exploiting the equivalent schematic representation of Fig. 7 that includes the spring, described by an equivalent mechanical stiffness k_m, the

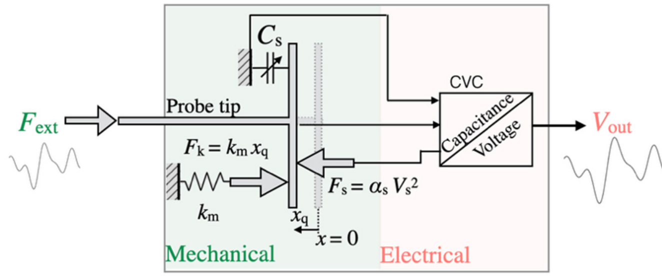

Fig. 7. Schematic representation of a typical capacitive MEMS force sensor based on open-loop configuration.

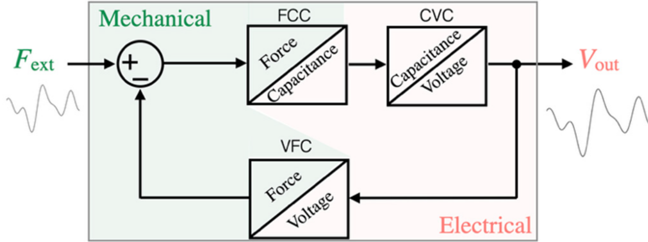

Fig. 8. Block diagram of a typical MEMS force sensor based on closed-loop configuration.

sensing capacitance C_s which is dependent of the position x_Q and the CVC. The CVC for stationary-mode force sensing usually exploits a sensing signal $v_s(t)$, characterized by an rms amplitude V_s and a frequency f_s, to generate a charge variation proportional to the capacitance variation that is than converted in an output voltage [41]. Due to the rms amplitude V_s the sensing signal induces an electrostatic force F_s that results:

$$|F_s| = \alpha_s V_s^2 \tag{8}$$

where, as described in (6) α_s is the electro-mechanical transduction factor related to the sensing capacitance C_s.

Assuming the forces as positive in the direction of the arrows in Fig. 7 the equilibrium of forces acting on the probe tip yields:

$$F_{ext} + F_k - F_s = 0 \tag{9}$$

where $F_k = k_m x_q$ is the mechanical force produced by the spring of the MEMS device whose stiffness k_m is assumed to be constant, i.e., position independent. Usually, the values of f_s and V_s are carefully selected to make F_s negligible compared to other forces acting on the probe tip [42]. The external force can thus be obtained by knowing the mechanical stiffness and by measuring the capacitance and in turn the displacement x_q.

B. Closed-Loop Configuration

Fig. 8 shows a schematic representation of a force sensor exploiting a closed-loop configuration. As for the open-loop described in Section III-A, the closed-loop configuration allows to obtain an electrical output signal V_{out} function of the mechanical input signal F_{ext}. However, the closed-loop configuration exploits force-feedback control to nullify the mechanical displacement of the movable mass of the device, directly transducing forces without requiring the displacement. Typically, the closed-loop configuration embeds a FCC and a CVC to convert F_{ext} from the mechanical domain into V_{out} in the electrical domain. The electrical output is then provided to the VFC in a negative-feedback mechanism to generate in the mechanical domain a force that counterbalances F_{ext} thus nulling the displacement and providing an ideally infinite input mechanical impedance. Fig. 9 shows examples of electrostatic-capacitive MEMS force sensors employed in closed-loop configuration. Fig. 9a shows the 3D CAD view of a MEMS based force sensor that has been fabricated and tested in both open-loop and closed-loop configuration [43]. In open-loop configuration the sensor force-position characteristic showed a dependency on the stiffness of the sensor flexures. Whereas, when tested in closed-loop configuration the sensor showed a virtually infinite stiffness thus allowing to extend the force measurement range up to 10 µN. Fig. 9b shows the experimental setup employed to test a MEMS force sensor with double actuator position-feedback mechanism [44]. The developed MEMS force sensor employed two distinct variable-area capacitors as VFC and a set of variable-gap capacitor as FCC.

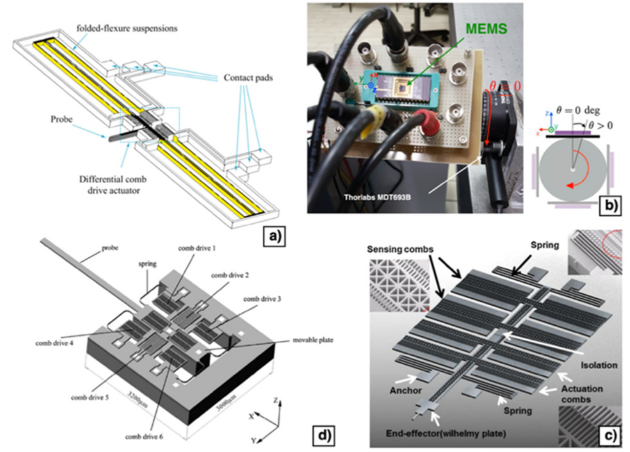

Fig. 9. Examples of electrostatic-capacitive MEMS force sensors available in literature based on closed-loop configuration: (**a**) 3D CAD view of a MEMS force sensor [43], (**b**) experimental setup employed to test a double-actuator position-feedback MEMS force sensor [44], (**c**) solid model of a MEMS force sensor with key parts identified [45] and (**d**) solid model of a two-axis microactuators employed in a real-time control loop [46].

The sensor has been successfully tested in the range from [-217, 226] down to [-20.5, 21.4] nN showing a force sensitivity of 2.34 up to 8.43 V/µN. Fig. 9c shows a solid model of a MEMS force sensor embedding electrostatic drivers for actuation and capacitive combs for displacement sensing [45]. The MEMS sensor has been adopted in a closed-loop configuration capable of regulating the position of the movable mass over a range of 40 µm with a 5 nm resolution and controlling forces up to 300 µN with a resolution of 25 nN. The MEMS sensor in closed-loop configuration has been employed to measure surface tension forces acting on a Wilhelmy plate tensiometer. Fig. 9d shows a solid model of a two-axis MEMS microactuators embedding a closed-loop system to extend the travel range avoiding the pull-in effect [46]. The fabricated device incorporates sets of parallel-plate capacitors, functioning as VFC and FCC, within a proportional-integral-derivative (PID) control loop to achieve the desired linear system response. Typically, electrostatic-capacitive MEMS force sensors, as the ones shown in Fig. 9, exhibit a probe tip suspended by springs on which F_{ext} is applied, a FCC and a VFC based on either variable-area or variable-gap capacitor.

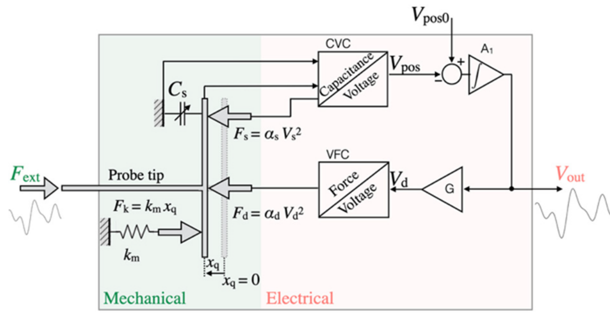

Fig. 10. Schematic representation of a typical electrostatic-capacitive MEMS force sensor based on closed-loop configuration.

These devices can thus be described by exploiting the equivalent schematic representation of Fig. 10. The schematic representation includes the spring, with mechanical stiffness k_m, the sensing capacitance C_s function of x_q and the CVC which exploits the sensing signal $v_s(t)$ to convert C_s into the voltage $V_{pos.}$ In closed-loop configuration, the position-dependent voltage V_{pos} is kept equal to the applied set-point voltage V_{pos0} by the feedback loop thanks to the ideally infinite DC-gain of the integrator amplifier A_1. The output voltage of the integrator amplifier V_{out} is provided to a voltage amplifier with gain G to properly drive with the voltage V_d a VFC. The generated electrostatic force F_d is then able to counterbalance F_{ext} and in turn nullify the mechanical displacement of the movable mass of the device. Assuming the forces as positive in the direction of the arrows in Fig. 10 the equilibrium of forces acting on the probe tip yields:

$$F_{ext} + F_k - F_s - F_d = 0. \tag{10}$$

The electrostatic force F_d can thus be employed to counterbalance F_{ext} and in turn allowing its measurement. Although closed-loop configuration provides enhanced performances in terms of stability and resolution in MEMS force sensor, feedback loop alone is typically not sufficient to remove the dependency of mechanical properties of the sensor, such as the spring stiffness or the set working position, on measurement range/sensitivity. To address these issues, advanced closed-loop based techniques have been developed. In [47] the dependency of the mechanical parameters has been removed by using a feedback signal to actuate a second set of transducers to counterbalance the applied force. Therefore, the range and sensitivity of the sensor become a function of actuator parameters thus allowing greater freedom in the design process and removing the need for the mechanical calibration. The possibility to make the sensitivity and range function of actuator parameters has been further investigated in [44]. The exploitation of two independent electrostatic actuators has allowed to obtain electrically adjustable force sensitivity and measurement range while being independent from the mechanical properties of the device such as the working position and the spring stiffness.

C. Comparison of Open-Loop and Closed-Loop Configuration

As described in Section III-A and III-B either open-loop or closed-loop configuration allow to transduce the mechanical signal, i.e. the external force, into an electrical signal, i.e., the output voltage. Therefore, both configurations are suitable to be implemented in MEMS force sensors. However, depending on the targeted application one configuration may offer advantages over the other in terms of sensitivity, bandwidth, linearity, power consumption, and overall system stability. The open-loop configuration typically exhibits several drawbacks such as the dependence on the measurement force range and the sensitivity from mechanical parameters, e.g., the spring stiffness. Specifically, spring stiffness can become position dependent at large deformations thus introducing nonlinearities and instabilities [48]. Furthermore, to derive the applied external force the displacement must be measured. By embedding capacitive sensor additional mechanical parameter dependency can be introduced thus leading to further non-linearities and undesired measurement range limitations. However, since open-loop configuration does not require force-feedback control systems, the sensor design can be simpler and easier to implement. The absence of components required to implement the force-feedback loop, e.g., external circuitry or VFCs, leads to lower costs, reduced power consumption and smaller size. The absence of feedback delays can possibly allow open-loop sensors to exhibit a lower response time to force changes, which can be advantageous in high-speed applications. Conversely, closed-loop configuration allows to maintain the MEMS mass at its initial position by means of a feedback signal employed to balance the applied force. This leads to a comprehensive solution that overcomes some of the disadvantages of an open-loop configuration since it provides more precise and reliable measurements while minimizing nonlinearities and improving accuracy [49]. By adopting closed-loop configuration the system becomes more robust to perturbations from mechanical vibrations, can measures dynamic and large-amplitude forces with better resolution and higher stability [50]. However, the enhancement of performances in terms of stability, measurement range and resolution are achieved at the expenses of a higher control system complexity, higher power consumption and bigger size.

Closed-loop configuration typically requires force-feedback control systems capable to set the MEMS mass position. Viable solutions have been proposed in the literature based on PID controller able to suppress undesired in-plane excitations [51] or to reduce the measurement noise [52]. These solutions effectively enhance the sensor performances in terms of resolution but restraint the MEMS sensor bandwidth. Other solutions able to bear the MEMS dynamics exploit digital control strategy based on sigma-delta modulator, which can preserve all advantages of closed-loop systems and concurrently produce a digital output in the format of a pulse density modulated bitstream [53].

Force-feedback control systems have been also employed to mitigate pull-in instability, a major limitation on the measurement range of capacitive MEMS sensors.

In literature several strategies have been proposed to overcome this limitation. A current driven approach has been proposed in [54] that allows to achieve full travel range for an electrostatic actuator up to five times the pull-in value. In [46] a nonlinear model inversion technique is proposed for nonlin-

TABLE I
COMPARISON OF POSSIBLE ADVANTAGES AND DISADVANTAGES OF OPEN-LOOP AND CLOSED-LOOP CONFIGURATION

	Advantages	**Disadvantages**
Open-loop configuration	- No external force-feedback control system required - Simpler MEMS design and smaller footprint - Lower production cost - Reduced power consumption - Faster response time and wider sensor bandwidth	- Force measurement range and force sensitivity depend on the MEMS mechanical parameters - Susceptible to nonlinearities and pull-in instabilities - Requires direct displacement measurement of the movable MEMS mass
Closed-loop configuration	- Reduced nonlinearities - More robust against mechanical vibrations - Enhanced resolution and long-term stability - Pull-in effect mitigated - Minimized force measurement range and force sensitivity dependency from MEMS mechanical parameters - No direct displacement measurement of the movable MEMS mass required	- External force-feedback control system required - Higher control system complexity - Higher power consumption - Larger overall MEMS size - Limited bandwidth and slower response time

TABLE II
COMPARISON OF THE PERFORMANCES OF CAPACITIVE-BASED MEMS FORCE SENSORS REPORTED IN LITERATURE

Ref.	**Publication year**	**Sensitivity**	**Estimated resolution**	**Measurement range**	**Configuration**
[61]	2002	-	0.01 µN	490 µN	Open-loop
[62]	2003	-	0.01 µN	25 µN	Open-loop
[63]	2005	1.35 mV/ µN	0.68 µN	± 1 mN	Open-loop
[60]	2006	25 V/µN	-	± 1.25 µN	Open-loop
[37]	2009	-	1.4 µN	1 mN	Open-loop
[40]	2010	0.02 fF/nN	2.8 pN	1 mN	Open-loop
[57]	2010	16 mV/µN	33.2 nN	110 µN	Open-loop
[58]	2010	-	500 pN	1 µN	Open-loop
[59]	2010	-	50 pN	1 µN	Open-loop
[38]	2013	-	0.4 µN	± 2 mN	Open-loop
[45]	2014	-	25 nN	300 µN	Closed-loop
[47]	2014	-	7.8 nN	1.5 mN	Closed-loop
[16]	2017	6 V/µN	5 nN	200 nN	Closed-loop
[43]	2019	-	50 µN	-	Closed-loop
[44]	2020	8.43 V/µN	345 pN	± 21.4 nN	Closed-loop
[65]	2020	-	4.74 nN	± 211.7 µN	Closed-loop
[39]	2023	0.529 aF/nN	0.4436 nN	13.83 µN	Open-loop
[66]	2023	5.04 fF/N	-	5 N	Open-loop
[64]	2023	-	10.12 nN	± 200 µN	Closed-loop
[49]	2024	-	4.67 nN	± 138.7 µN	Closed-loop

ear electrostatic micro actuation system to overcome pull-in instability thus enhancing the travel distance of transverse comb drive actuators. In [55] a control system able to increase the dynamic range and to allow operation of electrostatic micromirrors beyond the pull-in angle is presented.

Closed-loop configuration can improve the time stability of MEMS force sensors, which typically depends on the stability of their mechanical and electrical parameters. Charges trapped on the oxide layers of the electrodes can lead to electrostatic forces even in the absence of an external bias voltage.

The amount of trapped charge fluctuates over time thereby affecting the long-term stability of capacitive MEMS sensors. In [56] the electromechanical stability of commercial accelerometers was analyzed, and drift rates in the order of 0.01 %/h were reported.

Table I summarizes the advantages and disadvantages of open-loop and closed-loop configuration. The choice between the two configurations should be guided by a careful analysis of the specific performance requirements and design constraints of the intended MEMS sensing application.

Table II compares the performances in terms of sensitivity, resolution and measurement range of capacitive-based MEMS force sensors employed in open-loop and closed-loop configuration taken from the literature.

As shown in Table II capacitive-based MEMS force sensor can cover different measurement range up to units of N while having outstanding resolution down to units of pN.

The estimated resolution and the measurement range shown in Table II have been plotted as a function of the publication year in Fig. 11 and Fig. 12, respectively. The data shown from both figures highlight that open-loop configurations have been studied more in earlier years (2002 - 2013), with relatively fewer recent publications.

Conversely, closed-loop systems became more prominent after 2014, possibly indicating a shift in research likely due to improved robustness, control, and stability. Nevertheless, open-loop configurations allow to span different measurement range while providing remarkable resolution compared to closed-loop configurations.

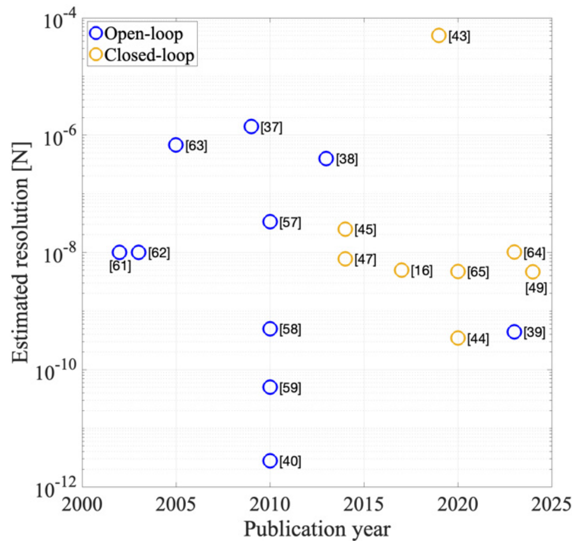

Fig. 11. Estimated resolution as a function of publication year of capacitive-based MEMS force sensors reported in Table II taken from the literature.

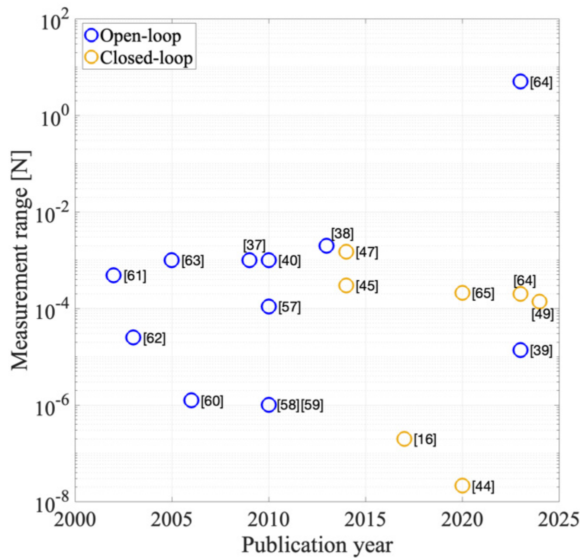

Fig. 12. Measurement range as a function of publication year of capacitive-based MEMS force sensors reported in Table II taken from the literature.

The latter appear more consistent in delivering resolutions within 10^{-9} - 10^{-8} N in the 10^{-4} - 10^{-3} N measurement range. This trend is also observable in Fig. 13 where a trade-off relationship between measurement range and resolution can be inferred.

IV. Conclusions and Perspectives

This paper has described a comprehensive review of the latest research developments focused on electrostatic-capacitive MEMS force sensors. At first, the review has summarized the most adopted transduction working principles employed for force sensing at the MEMS scale. Then, electrostatic-capacitive MEMS force sensors have been discussed in detail due to their advantage of being implementable in closed-loop configurations without the need for complex sensing structures or demanding actuation systems. These sensors can integrate both capacitive sensing and electrostatic actuation within a

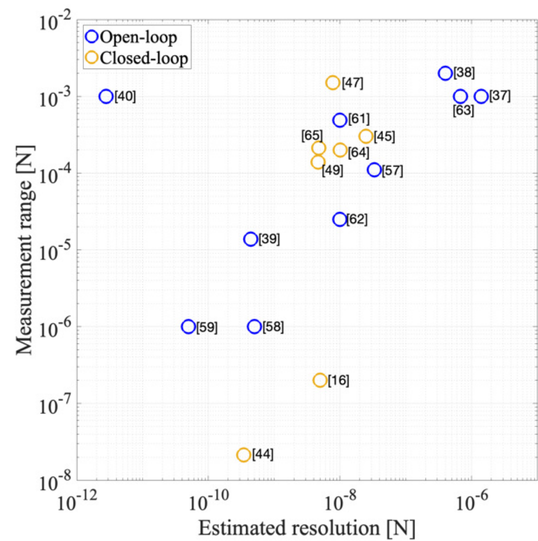

Fig. 13. Measurement range as a function of estimated resolution of capacitive-based MEMS force sensors reported in Table II taken from the literature.

single device, making the system compact and well-suited to be coupled with integrated circuits. The main building blocks employed in MEMS force sensors such as the Force-to-Capacitance Converter and the Voltage-to-Force Converter have been described by considering both variable-area and variable-gap configurations. The working principles of open-loop and closed-loop configurations have been detailed, with examples taken from the literature. Both configurations have been analyzed in terms of sensitivity, bandwidth, linearity, power consumption, and overall system stability. Their respective advantages and disadvantages have been examined. The open-loop configuration is more prone to non-linearities, inaccuracies, and pull-in instabilities but offers lower cost, reduced power consumption, and smaller size. In contrast, the closed-loop configuration is more robust against mechanical vibrations and provides improved accuracy at the expenses of higher system complexity, increased power consumption, larger size, and the need for precise tuning of the feedback loop during calibration.

Electrostatic-capacitive MEMS force sensors are expected to enhance their functionality across a broad range of applications. One promising direction is the ability to measure different physical quantities and combine them to enhance sensing capabilities. A single force sensor may simultaneously detect multiple physical parameters, such as stiffness and temperature, by leveraging on stacked materials or by integrating multiple sensing mechanisms in the microscale. This enables more compact and integrated solutions for wearable devices, robotics, and biological environment. In parallel, the exploitation of AI-enhanced signal processing may allow to overcome traditional limitations such as non-linearity or temperature drift. By embedding on-chip machine learning models future MEMS force sensors could perform real-time self-calibration, fault detection, and analysis of force signals. An untracked path is also multi-axis force sensing at the MEMS scale, which enables the measurement of force vectors rather than just scalar magnitudes. Although few examples

are already available in the literature, they often suffer from intrinsic non-linearities and complex calibration procedures. Advanced structural designs have the potential to enhance 3D force detection, which is critical for applications such as biomechanical monitoring and robotic manipulation.

Finally, there is a growing interest in improving closed-loop architectures by implementing self-tuning and fully digital feedback systems for robustness enhancement. Together, these advancements promise to renovate electrostatic-capacitive MEMS force sensors into multipurpose, and high-performance tools for next-generation sensing systems.

Acknowledgment

The author gratefully acknowledges the valuable support and constructive insights received from Prof. Marco Baù, Prof. Marco Ferrari, and Prof. Vittorio Ferrari.

References

[1] D. M. Stefanescu and M. A. Anghel, "Electrical methods for force measurement—A brief survey," *Measurement*, vol. 46, no. 2, pp. 949–959, Feb. 2013, doi: 10.1016/j.measurement.2012.10.020.

[2] B. E. Jones and T. Yan, "MEMS force and torque sensors/a review," *Meas. Control*, vol. 37, no. 8, pp. 236–241, Oct. 2004, doi: 10.1177/002029400403700801.

[3] A. Dhapte. (2025). *Force Sensor Market Research Report Information By Type, By Application and By Region-Industry Forecast Till 2032*. [Online]. Available: https://www.marketresearchfuture.com/reports/force-sensor-market-4454

[4] J. Bryzek et al., "Advanced IC sensors and microstructures for high-volume applications," *IEEE Circuit Device Mag.*, vol. 2006, pp. 8–21, Mar. 2006, doi: 10.1109/MCD.2006.1615241.

[5] Y. Qin, D. Wang, and Y. Yang, "Integrated cutting force measurement system based on MEMS sensor for monitoring milling process," *Microsyst. Technol.*, vol. 26, no. 6, pp. 2095–2104, Jun. 2020, doi: 10.1007/s00542-020-04768-y.

[6] M. Muroyama, H. Hirano, C. Shao, and S. Tanaka, "Development of a real-time force and temperature sensing system with MEMS-LSI integrated tactile sensors for next-generation robots," *J. Robot. Mechatronics*, vol. 32, no. 2, pp. 323–332, Apr. 2020, doi: 10.20965/jrm.2020.p0323.

[7] A. Nastro, M. Ferrari, and V. Ferrari, "MEMS inclinometer with tunable-sensitivity and segmented overlapping Allan variance analysis," in *Proc. AEIT Int. Annu. Conf. (AEIT)*, Sep. 2020, pp. 1–6, doi: 10.23919/AEIT50178.2020.9241160.

[8] M. Ghanam, T. Bilger, F. Goldschmidtboeing, and P. Woias, "MEMS self-packaged capacitive absolute pressure and force sensors for high-temperature application," in *Proc. IEEE Sensors*, Oct. 2022, pp. 1–4, doi: 10.1109/SENSORS52175.2022.9967300.

[9] K. Kim, X. Liu, Y. Zhang, and Y. Sun, "MicroNewton force-controlled manipulation of biomaterials using a monolithic MEMS microgripper with two-axis force feedback," in *Proc. IEEE Int. Conf. Robot. Autom.*, May 2008, pp. 3100–3105, doi: 10.1109/ROBOT.2008.4543682.

[10] O. Loh, A. Vaziri, and H. D. Espinosa, "The potential of MEMS for advancing experiments and modeling in cell mechanics," *Experim. Mech.*, vol. 49, no. 1, pp. 105–124, Feb. 2009, doi: 10.1007/s11340-007-9099-8.

[11] H. Takahashi, "MEMS-based micro sensors for measuring the tiny forces acting on insects," *Sensors*, vol. 22, no. 20, p. 8018, Oct. 2022, doi: 10.3390/s22208018.

[12] Y. Yang, M. Zhao, H. Yinguo, H. Zhang, N. Guo, and Y. Zheng, "Micro-force sensing techniques and traceable reference forces: A review," *Meas. Sci. Technol.*, vol. 33, no. 11, Nov. 2022, Art. no. 114010, doi: 10.1088/1361-6501/ac83e1.

[13] R. Kumar, S. Rab, B. D. Pant, and S. Maji, "Design, development and characterization of MEMS silicon diaphragm force sensor," *Vacuum*, vol. 153, pp. 211–216, Jul. 2018, doi: 10.1016/j.vacuum.2018.04.029.

[14] S. Kohyama et al., "Spring constant measurement using a MEMS force and displacement sensor utilizing paralleled piezoresistive cantilevers," *J. Micromech. Microeng.*, vol. 28, no. 4, Feb. 2018, Art. no. 045013, doi: 10.1088/1361-6439/aaabf7.

[15] Y. Shen, E. Winder, N. Xi, C. A. Pomeroy, and U. C. Wejinya, "Closed-loop optimal control-enabled piezoelectric microforce sensors," *IEEE/ASME Trans. Mechatronics*, vol. 11, no. 4, pp. 420–427, Aug. 2006, doi: 10.1109/TMECH.2006.878555.

[16] A. Nastro, M. Ferrari, V. Ferrari, A.-L. Russo, and R. Ardito, "MEMS force sensor with DDS-based position feedback and tunable sensitivity," in *Proc. IEEE SENSORS*, Oct. 2017, pp. 1–3, doi: 10.1109/ICSENS.2017.8234151.

[17] F. Cerini et al., "Electro-mechanical modelling and experimental characterization of a high-aspect-ratio electrostatic-capacitive MEMS device," *Sens. Actuators A, Phys.*, vol. 266, pp. 219–231, Oct. 2017, doi: 10.1016/j.sna.2017.07.048.

[18] P. M. Winter et al., "Piezoresistivity," in *Encyclopedia of Nanotechnology*, 2012, pp. 2111–2117.

[19] Y. Maeda, K. Terao, F. Shimokawa, and H. Takao, "A MEMS hardness sensor with reduced contact force dependence based on the reference plane concept aimed for medical applications," *Japanese J. Appl. Phys.*, vol. 55, no. 4S, Apr. 2016, Art. no. 04EF11, doi: 10.7567/jjap.55.04ef11.

[20] M. Zou et al., "Fiber-tip polymer clamped-beam probe for high-sensitivity nanoforce measurements," *Light, Sci. Appl.*, vol. 10, no. 1, pp. 1–12, Aug. 2021, doi: 10.1038/s41377-021-00611-9.

[21] K. Reck, E. V. Thomsen, and O. Hansen, "MEMS Bragg grating force sensor," *Opt. Exp.*, vol. 19, no. 20, p. 19190, Sep. 2011, doi: 10.1364/oe.19.019190.

[22] Q. Liang, D. Zhang, G. Coppola, Y. Wang, S. Wei, and Y. Ge, "Multi-dimensional MEMS/micro sensor for force and moment sensing: A review," *IEEE Sensors J.*, vol. 14, no. 8, pp. 2643–2657, Aug. 2014, doi: 10.1109/JSEN.2014.2313860.

[23] S.-K. Yeh, H.-C. Chang, and W. Fang, "Development of CMOS MEMS inductive type tactile sensor with the integration of chrome steel ball force interface," *J. Micromech. Microeng.*, vol. 28, no. 4, Feb. 2018, Art. no. 044005, doi: 10.1088/1361-6439/aaac24.

[24] Y. Sun and B. J. Nelson, "MEMS capacitive force sensors for cellular and flight biomechanics," *Biomed. Mater.*, vol. 2, no. 1, pp. S16–S22, Mar. 2007, doi: 10.1088/1748-6041/2/1/s03.

[25] C. A. Gutierrez and E. Meng, "Impedance-based force transduction within fluid-filled parylene microstructures," *J. Microelectromech. Syst.*, vol. 20, no. 5, pp. 1098–1108, Oct. 2011, doi: 10.1109/JMEMS.2011.2160935.

[26] B. J. Kim, C. A. Gutierrez, G. A. Gerhardt, and E. Meng, "Parylene-based electrochemical-MEMS force sensor array for assessing neural probe insertion mechanics," in *Proc. IEEE 25th Int. Conf. Micro Electro Mech. Syst. (MEMS)*, Jan. 2012, pp. 124–127, doi: 10.1109/MEMSYS.2012.6170109.

[27] (2024). *Introduction to Piezoelectric Force Sensors*. Accessed: Dec. 4, 2024. [Online]. Available: https://www.pcb.com/resources/technical-information/introduction-to-force-sensors

[28] J. Lee et al., "A micro-fabricated force sensor using an all thin film piezoelectric active sensor," *Sensors*, vol. 14, no. 12, pp. 22199–22207, Nov. 2014, doi: 10.3390/s141222199.

[29] H. Li et al., "A miniature layered SAW contact stress sensor for operation in cramped metallic slits," *Instrum. Experim. Techn.*, vol. 61, no. 4, pp. 610–617, Jul. 2018, doi: 10.1134/s0020441218040097.

[30] R. Hartansky et al., "Towards a MEMS force sensor via the electromagnetic principle," *Sensors*, vol. 23, no. 3, p. 1241, Jan. 2023, doi: 10.3390/s23031241.

[31] Y. Li et al., "Design and output characteristics of magnetostrictive tactile sensor for detecting force and stiffness of manipulated objects," *IEEE Trans. Ind. Informat.*, vol. 15, no. 2, pp. 1219–1225, Feb. 2019, doi: 10.1109/TII.2018.2862912.

[32] L. Weng, G. Xie, B. Zhang, W. Huang, B. Wang, and Z. Deng, "Magnetostrictive tactile sensor array for force and stiffness detection," *J. Magn. Magn. Mater.*, vol. 513, Nov. 2020, Art. no. 167068, doi: 10.1016/j.jmmm.2020.167068.

[33] H. Xin, M. Andraud, P. Baltus, E. Cantatore, and P. Harpe, "A 0.1-nW–1-μ w energy-efficient all-dynamic versatile capacitance-to-digital converter," *IEEE J. Solid-State Circuits*, vol. 54, no. 7, pp. 1841–1851, Jul. 2019, doi: 10.1109/JSSC.2019.2902754.

[34] J. Fraden, *Handbook of Modern Sensors: Physics, Designs, and Applications*, 3rd ed., San Diego, CA, USA: Advanced Monitors Corp., 2003.

[35] R. Ardito, A. Frangi, A. Corigliano, B. De Masi, and G. Cazzaniga, "The effect of nano-scale interaction forces on the premature pull-in of real-life micro-electro-mechanical systems," *Microelectron. Rel.*, vol. 52, no. 1, pp. 271–281, Jan. 2012, doi: 10.1016/j.microrel.2011.08.021.

[36] B. Jakoby, "On the origin and the calculation of the force in electrostatic actuators," *Eur. J. Phys.*, vol. 37, no. 4, May 2016, Art. no. 045207, doi: 10.1088/0143-0807/37/4/045207.

[37] F. Beyeler, S. Muntwyler, and B. J. Nelson, "A six-axis MEMS force–torque sensor with micro-Newton and nano-newtonmeter resolution," *J. Microelectromech. Syst.*, vol. 18, no. 2, pp. 433–441, Apr. 2009, doi: 10.1109/JMEMS.2009.2013387.

[38] W. Chen, J. Jiang, J. Liu, and W. Chen, "A MEMS based sensor for large scale force measurement," in *Proc. IEEE/ASME Int. Conf. Adv. Intell. Mechatronics*, Jul. 2013, pp. 1278–1283, doi: 10.1109/AIM.2013.6584270.

[39] W. Gao et al., "A high-resolution MEMS capacitive force sensor with bionic swallow comb arrays for ultralow multiphysics measurement," *IEEE Trans. Ind. Electron.*, vol. 70, no. 7, pp. 7467–7477, Jul. 2023, doi: 10.1109/TIE.2022.3203756.

[40] M. Haris and H. Qu, "A CMOS-MEMS nano-Newton force sensor for biomedical applications," in *Proc. IEEE 5th Int. Conf. Nano/Micro Engineered Mol. Syst.*, Jan. 2010, pp. 177–181, doi: 10.1109/NEMS.2010.5592177.

[41] F. Han, Q. Wu, R. Zhang, and J. Dong, "Capacitive sensor interface for an electrostatically levitated micromotor," *IEEE Trans. Instrum. Meas.*, vol. 58, no. 10, pp. 3519–3526, Oct. 2009, doi: 10.1109/TIM.2009.2018006.

[42] A. Nastro, M. Ferrari, and V. Ferrari, "Electrostatic-capacitive MEMS stiffness sensor with position-feedback mechanism," in *Proc. IEEE Sensors*, Oct. 2021, pp. 1–4, doi: 10.1109/SENSORS47087.2021.9639705.

[43] J. Cailliez, M. Boudaoud, A. Mohand-Ousaid, A. Weill–Duflos, S. Haliyo, and S. Régnier, "Modeling and experimental characterization of an active MEMS based force sensor," *J. Micro-Bio Robot.*, vol. 15, no. 1, pp. 53–64, Jun. 2019, doi: 10.1007/s12213-019-00115-1.

[44] A. Nastro, M. Ferrari, and V. Ferrari, "Double-actuator position-feedback mechanism for adjustable sensitivity in electrostatic-capacitive MEMS force sensors," *Sens. Actuators A, Phys.*, vol. 312, Sep. 2020, Art. no. 112127, doi: 10.1016/j.sna.2020.112127.

[45] B. Koo and P. M. Ferreira, "An active MEMS probe for fine position and force measurements," *Precis. Eng.*, vol. 38, no. 4, pp. 738–748, Oct. 2014, doi: 10.1016/j.precisioneng.2014.03.010.

[46] Y. Sun, D. Piyabongkarn, A. Sezen, B. J. Nelson, and R. Rajamani, "A high-aspect-ratio two-axis electrostatic microactuator with extended travel range," *Sens. Actuators A, Phys.*, vol. 102, nos. 1–2, pp. 49–60, Dec. 2002, doi: 10.1016/s0924-4247(02)00298-4.

[47] M. Bulut Coskun, S. Moore, S. O. R. Moheimani, A. Neild, and T. Alan, "Zero displacement microelectromechanical force sensor using feedback control," *Appl. Phys. Lett.*, vol. 104, no. 15, Apr. 2014, Art. no. 153502, doi: 10.1063/1.4871380.

[48] B. Vysotskyi, F. Parrain, D. Aubry, P. Gaucher, X. Le Roux, and E. Lefeuvre, "Engineering the structural nonlinearity using multimodal-shaped springs in MEMS," *J. Microelectromech. Syst.*, vol. 27, no. 1, pp. 40–46, Feb. 2018, doi: 10.1109/JMEMS.2017.2779179.

[49] D. Dadkhah and S. O. R. Moheimani, "Design, fabrication, and control of a double-stage MEMS force sensor," *IEEE/ASME Trans. Mechatronics*, vol. 30, no. 3, pp. 1819–1829, Jun. 2025, doi: 10.1109/TMECH.2024.3409458.

[50] D. Dadkhah and S. O. R. Moheimani, "Combining H_∞ and resonant control to enable high-bandwidth measurements with a MEMS force sensor," *Mechatronics*, vol. 96, Dec. 2023, Art. no. 103086, doi: 10.1016/j.mechatronics.2023.103086.

[51] R. J. Mozhdehi and A. S. Ghafari, "Optimal PID control of a nano-Newton CMOS-MEMS capacitive force sensor for biomedical applications," *Mech. Ind.*, vol. 15, no. 2, pp. 139–145, 2014, doi: 10.1051/meca/2014019.

[52] E. Ranjbar, M. B. Menhaj, A. A. Suratgar, J. Andreu-Perez, and M. Prasad, "Design of a fuzzy PID controller for a MEMS tunable capacitor for noise reduction in a voltage reference source," *Social Netw. Appl. Sci.*, vol. 3, no. 6, pp. 1–17, Jun. 2021, doi: 10.1007/s42452-021-04585-6.

[53] F. Chen, X. Li, and M. Kraft, "Electromechanical sigma–delta modulators (ΣΔM) force feedback interfaces for capacitive MEMS inertial sensors: A review," *IEEE Sensors J.*, vol. 16, no. 17, pp. 6476–6495, Sep. 2016, doi: 10.1109/JSEN.2016.2582198.

[54] R. Nadal-Guardia, A. Dehe, R. Aigner, and L. M. Castaner, "Current drive methods to extend the range of travel of electrostatic microactuators beyond the voltage pull-in point," *J. Microelectromech. Syst.*, vol. 11, no. 3, pp. 255–263, Jun. 2002, doi: 10.1109/JMEMS.2002.1007404.

[55] J. Chen, W. Weingartner, A. Azarov, and R. C. Giles, "Tilt-angle stabilization of electrostatically actuated micromechanical mirrors beyond the pull-in point," *J. Microelectromech. Syst.*, vol. 13, no. 6, pp. 988–997, Dec. 2004, doi: 10.1109/JMEMS.2004.838391.

[56] A. Oja, J. Kyynarainen, and H. Seppa, "Electromechanical stability of capacitive transducers," *Proc. SPIE*, vol. 4408, pp. 463–468, Apr. 2001, doi: 10.1117/12.425379.

[57] K. Kim, J. Cheng, Q. Liu, X. Y. Wu, and Y. Sun, "Investigation of mechanical properties of soft hydrogel microcapsules in relation to protein delivery using a MEMS force sensor," *J. Biomed. Mater. Res. A*, vol. 92, no. 1, pp. 103–113, Jan. 2010, doi: 10.1002/jbm.a.32338.

[58] J. Rajagopalan, A. Tofangchi, and M. T. A. Saif, "Highly linear, ultra sensitive bio-MEMS force sensors with large force measurement range," in *Proc. IEEE 23rd Int. Conf. Micro Electro Mech. Syst. (MEMS)*, Jan. 2010, pp. 88–91, doi: 10.1109/MEMSYS.2010.5442558.

[59] J. Rajagopalan, A. Tofangchi, and M. T. A. Saif, "Linear high-resolution BioMEMS force sensors with large measurement range," *J. Microelectromech. Syst.*, vol. 19, no. 6, pp. 1380–1389, Dec. 2010, doi: 10.1109/JMEMS.2010.2076780.

[60] Y. Sun, K. Kim, R. M. Voyles, and B. J. Nelson, "Calibration of multi-axis MEMS force sensors using the shape from motion method," in *Proc. IEEE Int. Conf. Robot. Autom., ICRA.*, Jul. 2006, pp. 269–274, doi: 10.1109/ROBOT.2006.1641723.

[61] Y. Sun, B. J. Nelson, D. P. Potasek, and E. Enikov, "A bulk microfabricated multi-axis capacitive cellular force sensor using transverse comb drives," *J. Micromech. Microeng.*, vol. 12, no. 6, pp. 832–840, Nov. 2002, doi: 10.1088/0960-1317/12/6/314.

[62] Y. Sun, K.-T. Wan, K. P. Roberts, J. C. Bischof, and B. J. Nelson, "Mechanical property characterization of mouse zona pellucida," *IEEE Trans. Nanobiosci.*, vol. 2, no. 4, pp. 279–286, Dec. 2003, doi: 10.1109/TNB.2003.820273.

[63] Y. Sun, S. N. Fry, D. P. Potasek, D. J. Bell, and B. J. Nelson, "Characterizing fruit fly flight behavior using a microforce sensor with a new comb-drive configuration," *J. Microelectromech. Syst.*, vol. 14, no. 1, pp. 4–11, Feb. 2005, doi: 10.1109/JMEMS.2004.839028.

[64] D. Dadkhah and S. O. Reza Moheimani, "A high-bandwidth closed-loop MEMS force sensor with system dynamics adjustment," in *Proc. IEEE/ASME Int. Conf. Adv. Intell. Mechatronics (AIM)*, Jun. 2023, pp. 79–84, doi: 10.1109/AIM46323.2023.10196208.

[65] M. Maroufi, H. Alemansour, and S. O. R. Moheimani, "A high dynamic range closed-loop stiffness-adjustable MEMS force sensor," *J. Microelectromech. Syst.*, vol. 29, no. 3, pp. 397–407, Jun. 2020, doi: 10.1109/JMEMS.2020.2983193.

[66] Y. Huang, Y.-L. Chen, S. Lin, F. Shih, Z. Hu, and W. Fang, "Vertical integration of force transmission structure on capacitive CMOS-MEMS tactile force sensor for sensitivity improvement," in *Proc. IEEE 36th Int. Conf. Micro Electro Mech. Syst. (MEMS)*, Jan. 2023, pp. 791–794, doi: 10.1109/MEMS49605.2023.10052308.

Alessandro Nastro (Member, IEEE) was born in Romano di Lombardia, Italy, in 1991. He received the master's degree (cum laude) in electronics engineering and the Europaeus Ph.D. degree in information engineering from the University of Brescia in 2016 and 2020, respectively. Since 2019, he has been a Research Fellow in electronics and since May 2022, he has been an Assistant Professor with the Department of Information Engineering, University of Brescia. His research activity deals with the development of electronic techniques and circuits coupled to MEMS for static and dynamic micromechanical sensing and actuation. He has co-authored more than 50 publications in international peer-reviewed journals and international and national conference proceedings. He was the Session Chair of the conferences IEEE Sensors 2024 and IEEE SAS 2025. He has been assigned as a Guest Editor of a special issue in *Sensors* regarding MEMS devices.